Hindawi
International Journal of Aerospace Engineering
Volume 2022, Article ID 9307837, 14 pages
https://doi.org/10.1155/2022/9307837

Research Article

Self-Organizing Method on Mission-Level Task Allocation of Large-Scale Remote Sensing Satellite Swarm

Yang Jiang[1], **Yuan Gao**[2], **Longjiang Yu**[1], **Jing Yu**[1], **Yuting Li**[1] and **Hongtao Gao**[1]

[1]*Institute of Remote Sensing Satellite, China Academy of Space Technology, Beijing 100094, China*
[2]*Shanghai Electro-Mechanical Engineering Institute, Shanghai Academy of Spaceflight Technology, Shanghai 201109, China*

Correspondence should be addressed to Longjiang Yu; likeherod@163.com

Received 11 August 2021; Revised 18 June 2022; Accepted 15 July 2022; Published 1 September 2022

Academic Editor: Shaoming He

Distributed self-organization and self-management is an ideal way to achieve an autonomous and efficient operation of large-scale remote sensing satellite swarm. A distributed task allocation method based on the improved contract network algorithm is designed, orienting typical mission-level tasks. And the satellite swarm task allocation and planning model of potential target searching, moving target tracking, and sensitive target feature confirmation is given. The model is composed of observation requirement generation, observing area decomposition, and task allocation between different satellites. Simulation results confirm that the improved contract network algorithm can optimally solve the problem of mission-level task allocation autonomously in distributed swarm. This paper verifies that the self-organization method has the potential for engineering applications with simple realization theory and high calculation efficiency.

1. Introduction

Space-based earth observing system is developing from a small number of high-cost satellites to a large scale of swarm-satellites [1], with continuous cost reduction of satellite manufacture and launching. A satellite swarm refers to a decentralized control system of satellites that consists of multiple satellites with different orbit types, payloads, onboard resources, and platform capabilities [2]. The swarm members have to exchange information in accordance with standard communication protocols. The observing tasks are collected onboard or on the ground, exchanged through intersatellites and satellite-ground communication link, and finally executed by a group of satellites in the swarm.

The increasing number of satellites on orbit can enhance the overall application capabilities of the swarm system [3], while it also brings new obstacles in the operation of the system, such as

(i) ground system's operating difficulties caused by the large number of satellites

(ii) satellites' cooperation difficulties caused by the complexity of information exchanging in a dynamic environment

(iii) task allocation and planning difficulties caused by the complexity of diverse mission-level tasks

Hence, mission-level task allocation of large-scale satellite swarm remains to be researched. There are many researches on multisatellite task planning and management and on satellite data processing, and great progress has also been made in engineering. Aiming at the issues of swarm task allocation, the early research mainly focused on the centralized planning method on the ground. Considering multisatellite cooperation planning under emergency conditions, Chuan et al. proposed a multisatellite cooperative planning algorithm based on particle swarm optimization (PSO) algorithm combined with a heuristic algorithm [4]. Yingwu et al. proposed an evolutionary learning ant colony algorithm for multisatellite task planning [5]. Chao et al. established a multisatellite and multiobjective mission planning model

for agile satellites and proposed a hybrid parallel algorithm of generic and simulated annealing algorithm based on similarity and aggregation [6, 7]. Xiaolu et al. proposed an adaptive large neighborhood search algorithm for coordinated planning of multiple agile satellites [8]. Chuanqi et al. proposed an algorithm based on the improved genetic algorithm with elitist retention strategy that is used for mission planning of small satellite constellation [9]. These methods solved the task assignment issues of a constellation with small number of satellites and improved the response ability of satellite to unexpected observation tasks. But these studies are still difficult to apply to large-scale, heterogeneous satellite swarm.

To meet the requirements of heterogeneous satellite swarm task planning, distributed allocation methods were proposed. Huicheng et al. proposed a dynamic task allocation method for agile satellite constellation based on multiagent theory and introduced the contract network mechanism into the algorithm process [10]. Yitao et al. further developed an autonomous task planning method based on the bidding mechanism [11]. Longjiang et al. established a distributed collaborative task allocation model for agile satellite constellation [12]. The studies mentioned above improve the contract network algorithm; proposed task interaction strategies such as buying, selling, exchanging, and replacement; and improved the efficiency of constellation task allocation. However, most of the existing research does not model and simulate typical task scenarios; hence, there is still a gap between practical engineering applications.

Compared to a single-satellite task, swarm-oriented tasks are more abstract, macroscopic, and complex, which can be seen from potential target searching task, moving target tracking task, and sensitive target feature confirmation task [13–16]. The planning process of these mission-level tasks is mainly manifested as the autonomous mission transferring, negotiation, and assignment process among satellites, which can be defined as "self-organizing assignment of swarm missions." We further improve the distributed task allocation method of swarm based on the contract network algorithm, apply it to the complex task planning, and explore the method in the task allocation efficiency and task execution effect. The task allocation and planning are mainly discussed, and there remains further works to be done for engineering practice of remote sensing. For instance, image processing in diverse weather conditions [17, 18].

This paper is divided into five sections. A description of the remote sensing satellite swarm missions is given in Section 2. The distributed self-organizing method based on the improved contract network and the task allocation models orienting three typical mission-level tasks are presented in Section 3. The numerical simulations that demonstrate the feasibility of the designed method in three scenarios are performed in Section 4. And Section 5 gives a conclusion of the work.

2. Typical Mission-Level Task Description

For large-scale remote sensing satellite swarm, its structural characteristics are heterogeneous, distributed, and self-organized. The swarm (including its subgroups) can complete tasks that a single satellite cannot, especially some complex tasks.

Compared to a single satellite, the observation tasks faced by the remote sensing satellite swarm are more macroscopic, requiring multiple types of satellites to execute in time sequence, which can be defined as "mission-level" tasks. The swarm can decompose and allocate mission-level tasks as a whole, adjust tasks dynamically as the swarm status evolves, and finally form a task sequence executed by multiple satellites in an orderly manner in time. Three typical mission-level tasks are discussed as follows:

(1) Potential target searching task

Potential target searching task is proposed to search for certain targets in a specific area and find qualified targets as quickly as possible or find as many targets as possible within the specified time, as shown in Figure 1. The specific imaging tasks are planned and executed according to the strategy which based on the terrain, target characteristics, and other information of the area.

(2) Moving target tracking task

The moving target tracking task is proposed to continuously track the whole process of the movement of target from the start point to the end point, to ensure that the target position is always within the observable range and to prevent the target from being lost and restarting the target searching task, as shown in Figure 2. Predict next position range of the target from certain start position and then plan and execute the follow-up observations. The satellite needs to constantly adjust the parameters in the tracking process according to the actual target position and the predicted target position to ensure that the target is always in the detectable area.

(3) Sensitive target task

A sensitive target task is proposed to obtain multidimensional feature information of the target within a specific time window to improve the accuracy of target recognition. The constellation enables the target to be observed multiple times by multiple types of payloads within a period of time, through task planning and allocating, until observation elements of the target are all obtained, and its characteristic attributes are confirmed with a high degree of certainty, as shown in Figure 3. The task completion time is usually an important constraint to ensure the effectiveness of the information obtained. Moreover, the closer the imaging time of multiple types of payloads is, the higher the time correlation and the higher the value of the fusion image can get.

3. Distributed Task Self-Organizing Method of Remote Sensing Swarm

3.1. Swarm Distributed Task Allocation Scheme Architecture. From a principle point of view, the essence of swarm task allocation is the process of gradual decomposition and

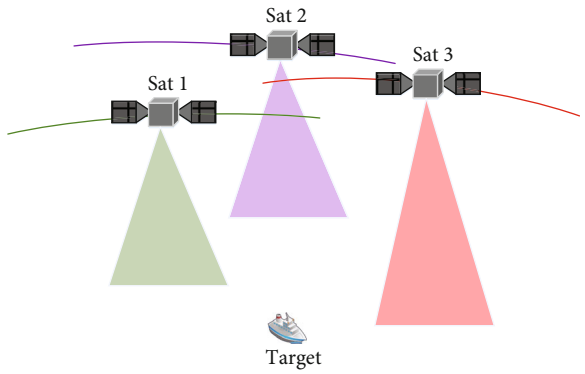

Figure 1: Potential target searching task mode scheme.

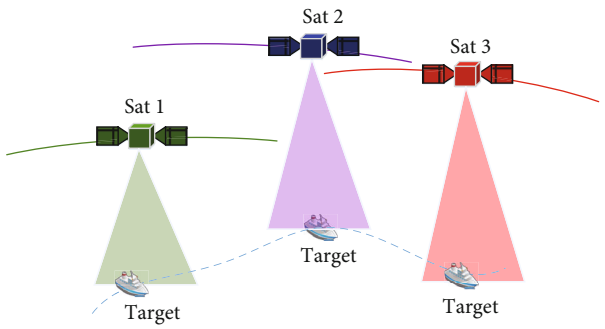

Figure 2: Moving target tracking task mode scheme.

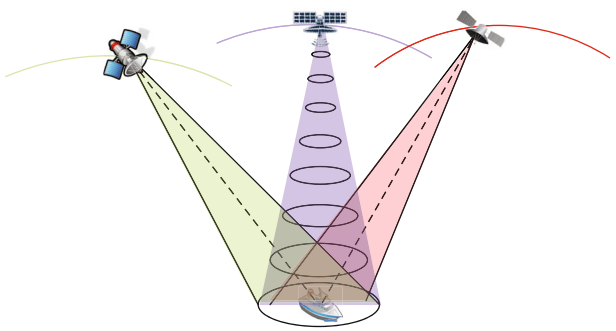

Figure 3: Sensitive target feature confirmation task mode scheme.

mapping of observation requirements among requirement space, task space, and execution space, as shown in Figure 4. The swarm task planning system receives multisource and multicategory observation requirements, forming a requirement space. The mission-level tasks can be classified into different types according to different kinds of targets, observation purposes, and so on, mentioned in Section 2. The ground or single satellite decomposes the requirements according to specific rules (target location, target acquisition period, observation elements, etc.) to generate tasks to be planned with more specific requirements to form a task space. By performing the arrangement of tasks to be planned to the satellites in space (that is, allocation and planning algorithms), the reasonable allocation of multitasks to multisatellites is completed, and the metatask sequence of each satellite is generated.

The distributed task negotiation mechanism is a core mechanism for realizing the mapping of swarm tasks from task space to execution space, and its foundation is the theory of the multiagent system. The remote sensing satellite in the swarm is a typical type of agent, which has the characteristics of high autonomy, strong dynamic, and concurrent behavior. Considering a centralized planner on the ground is used to perform global planning, the search space will be greatly expanded and difficult to solve. The distributed structure is a more ideal structure for agent organizations.

3.2. Intersatellite Task Allocation Algorithm Based on Improved Contract Network. The distributed task allocation method based on the improved contract network algorithm is adopted to realize the optimal allocation of intersatellite tasks, that is, to realize the mapping of swarm tasks from task space to execution space.

After a certain master satellite is determined in a certain event, for satellites with communication conditions between the satellites, the master satellite can initiate the process of intersatellite task negotiation and allocation and iteratively complete task allocation according to the process of bidding, bid evaluation, bid winning, and confirmation [19, 20]. For different observation events, each satellite can act as the master satellite of a certain event, thereby initiating the negotiation and allocation process. Therefore, a single satellite can serve as both the master and slave at a specific moment.

The traditional contract network algorithm adopts the method of "sales contract," which has the limitation that the distribution result is easy to fall into the local optimum, and a single sales contract has insufficient processing capacity for the complex dynamic environment. In order to reinforce the solution processing capabilities of the contract network algorithm, three contract interaction methods, namely, sales contracts, exchange contracts, and replacement contracts, are used for task allocation to achieve better application effects. The negotiation of contract among swarm members is shown in Figure 5, and the contract is proceeded by members is shown in Figure 6.

(1) Contract sale

It is assumed that all tasks to be planned in the initial state are executed by the master satellite S_i in the process of allocating tasks. Contract sale means that the master satellite S_i assigns a task to be planned T_k^i to a slave satellite S_j through negotiation, so as to achieve a higher overall efficiency after allocation. The detailed steps are as follows:

(i) Step 1: the master satellite (auctioneer) S_i announces a task T_k^i from its task sequences to the market, using intersatellite communication to broadcast a tender invitation of the task

(ii) Step 2: after S_j received the auction information of the task T_k^i, self-efficiency variance produced in task execution can be calculated by

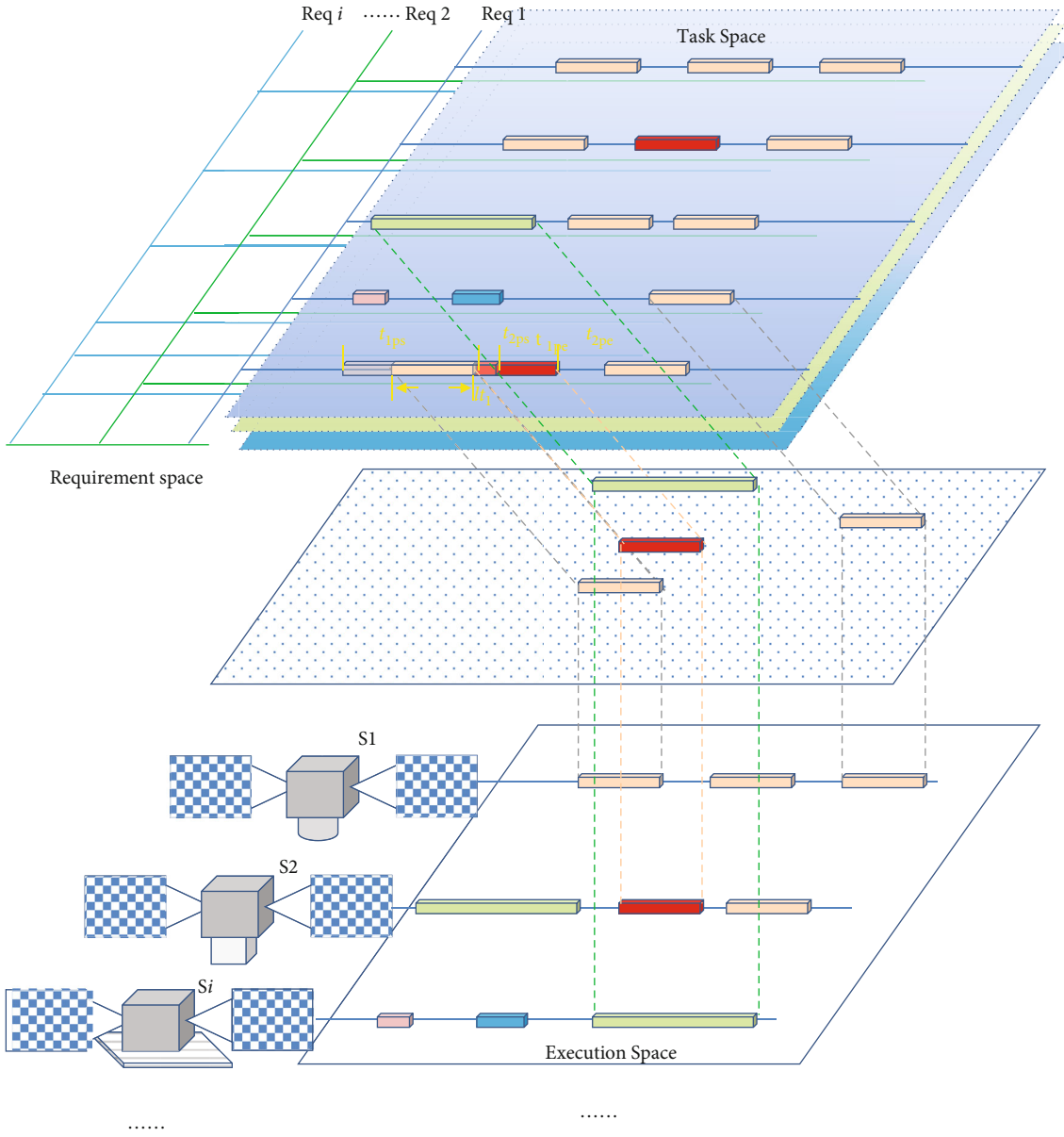

Figure 4: Swarm task allocation process model diagram.

$$\Delta I_j^+\left(T_k^i\right) = I_j\left(S_j \cup \left\{T_k^i\right\}\right) - I_j\left(S_j\right) \tag{1}$$

(i) Step 3: a bidding intention is sent to the auctioneer S_i from S_j when $\Delta I_j^+(T_k^i) > 0$

(ii) Step 4: after receiving the tender information, S_i starts calculating the change in overall efficiency $\Delta I_{i,j}^{\text{sale}}(T_k^i)$ of the system after accepting the biding, which can be obtained by

$$\Delta I_{i,j}^{\text{sale}}\left(T_k^i\right) = \Delta I_j^+\left(T_k^i\right) \tag{2}$$

(i) Step 5: the contract is signed and the task is transmitted to S_j for execution, if S_j can maximize the overall efficiency (has the greatest variation value $\Delta I_{i,j}^{\text{sale}}(T_k^i)_{\max}$)

(2) Contract exchange

Contract exchange means that after the slave satellite S_j gets a task to be planned T_k^i; it replaces its original task T_l^j to be executed and gives T_l^j to the master satellite S_i for execution, so as to obtain a higher overall efficiency. The detailed steps are as follows:

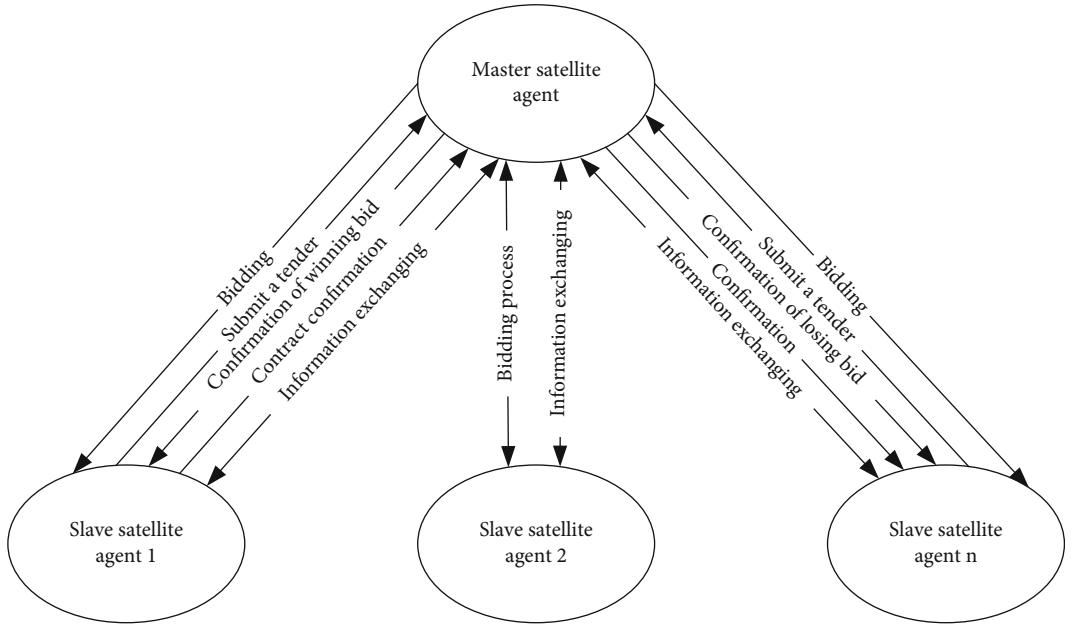

Figure 5: Task negotiation and allocation process based on contract net algorithm.

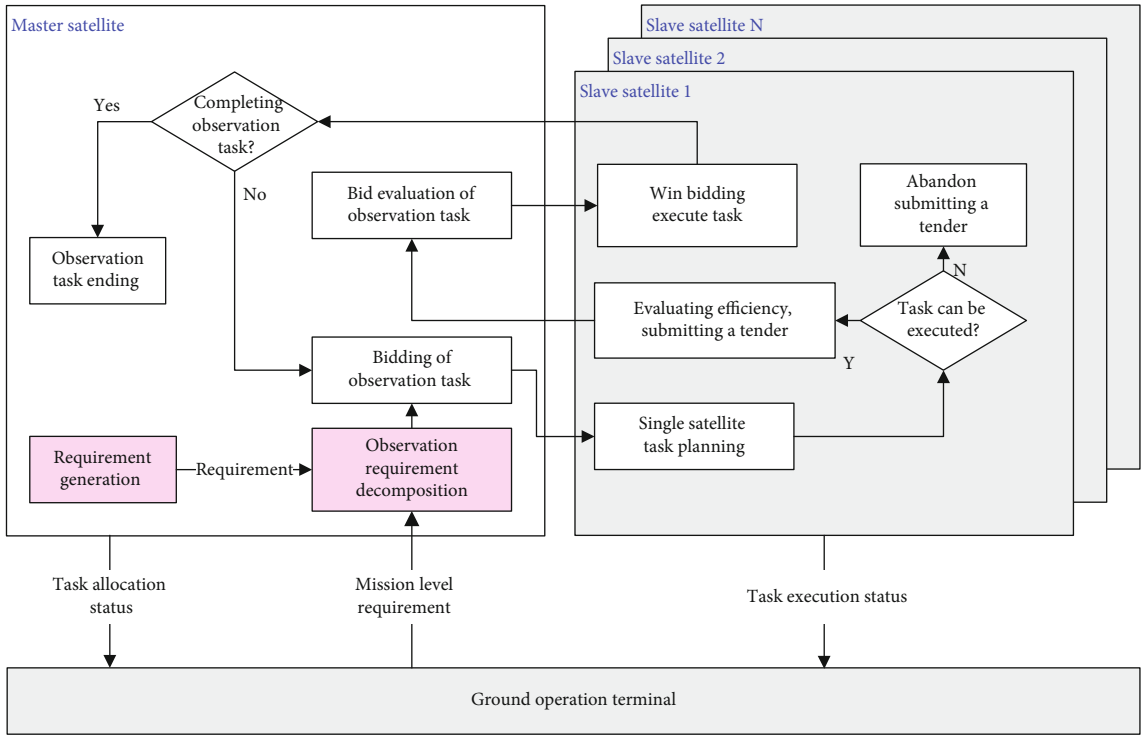

Figure 6: Swarm collaborative task allocation and planning process.

(i) Step 1: contract exchange starts when S_j cannot propose a valid bidding intention, after receiving the bidding announcement of task T_k^i from S_i

(ii) Step 2: S_i proposes to exchange its task T_l^j with task T_k^i, meanwhile, calculates the self-efficiency variance produced in task exchange by

$$\Delta I_j^{\text{swap}}\left(T_k^i, T_l^j\right) = I_j\left(S_j \cup \left\{T_k^i\right\}\right) \setminus \left\{T_l^j\right\} - I_j\left(S_j\right) \quad (3)$$

(i) Step 3: obtain the variance of self-efficiency and overall efficiency by the following equations after the exchange is realized, if S_i accepts the tender:

$$\Delta I_i^{\text{swap}}\left(T_k^i, T_l^j\right) = I_i\left(S_i \cup \left\{T_l^j\right\}\right) - I_i(S_i),$$
$$\Delta I_{i,j}^{\text{swap}}\left(T_k^i, T_l^j\right) = \Delta I_i^{\text{swap}}\left(T_k^i, T_l^j\right) + \Delta I_j^{\text{swap}}\left(T_k^i, T_l^j\right) \tag{4}$$

(i) Step 4: the contract exchange is established if $\Delta I_{i,j}^{\text{swap}}(T_k^i, T_l^j) > 0$, and the overall efficiency can be maximized among all bids in this round

(3) Contract replacement

Contract replacement means that after the slave satellite S_j gets a task to be planned T_k^i, it replaces its original task to be executed T_l^j and directly obtains a higher overall efficiency; the slave satellite S_j can initiate a negotiated allocation mechanism and allocate this task to other slave satellites such as S_k for execution, thereby further increasing the overall revenue. The detailed steps are as follows:

(i) Step 1: contract replacement is only selected when S_j cannot propose a contract of sale, and the proposed contract of exchange is not accepted

(ii) Step 2: the variance of self-efficiency and overall efficiency after replacement is calculated by

$$\Delta I_j^{\text{replace}}\left(T_k^i, T_l^j\right) = I_j\left(\left(S_j \cup \left\{T_k^i\right\}\right) \setminus \left\{T_l^j\right\} - I_j(S_j),$$
$$\Delta I_{i,j}^{\text{replace}}\left(T_k^i, T_l^j\right) = \Delta I_j^{\text{replace}}\left(T_k^i, T_l^j\right) \tag{5}$$

(i) Step 3: the contract replacement is established if $\Delta I_{i,j}^{\text{replace}}(T_k^i, T_l^j) > 0$, and the overall efficiency can be maximized among all bids in this round

Using this algorithm framework, a mission-level task collaborative allocation and planning process is designed, including potential target searching, moving target tracking, and sensitive target feature confirmation. The contract network allocation part of the three types of algorithm processes is exactly the same. The difference lies in the observation requirement generation and the observation task decomposition part, that is, the task-level observation requirement is generated according to specific rules for the task to be planned.

3.3. Fundamental Algorithms in Task Allocation Model

3.3.1. Constraint Model. There are various constraints in multisatellite task allocation, and setting constraints reasonably can reduce the solution complexity with high model practicability. The variable notations are divided into satellite space and task space which are integrated in Table 1.

Assume tasks is $T_i \in T, 0 < i < N_T$ (N_T is the number of tasks to be planned in the collection), satellite $S_j \in S, 0 < i < N_S$ (N_S is the number of satellites in allocation system), the constrains in two aspect is as follows:

(1) Satellite part

(i) Resource constraint: the real-time S_j energy needs to be higher than the minimum allowable energy $E_{S-\min}$ during complete task collection T_{Sj} process, and lower than nominal energy $E_{S-\max}$; the amount of data should not exceed storage

$$E_{S-\min} < E_{Sj} < E_{S-\max},$$
$$G_{Sj} < G_{S-\max} \tag{6}$$

(ii) Attitude range constraint: satellite attitude in anytime At_i must be within the possible attitude of the satellite and meet the requirement of incidence angle:

$$|\text{At}_i| \le |\text{At}| \tag{7}$$

(iii) Attitude maneuvering time constraint: Figure 7 is the schematic diagram of attitude maneuver between neighbor tasks. The attitude maneuver must not exceed the maneuverable limit between tasks, during S_j complete task collection T_{Sj} process:

$$(t_{Ac})_{i-1}^i \ge (t_{Ac-\min})_{i-1}^i, i-1>0,$$
$$(t_{Ac})_i^{i+1} \ge (t_{Ac-\min})_i^{i+1}, \tag{8}$$

where $(t_{Ac})_{i-1}^i$ is the maneuvering time from task T_{Sj}^{i-1} to $T_{Sj}^i$and$t_{Ac-\min}$is the maneuvering time correspond to maximum maneuvering power between neighbor tasks

(iv) Camera working time constraint: the time for S_j to complete task collection T_{Sj} must not exceed the limit imaging time

$$\sum_{i=1}^{N_T} \Delta t_i \le t_{w-\max} \cdot n_o, \tag{9}$$

where Δt_i is the imaging time for task T_i and n_o denotes the number of orbits which the task collection T_{Sj} distribute

Table 1: Variable names and representation notations.

Satellite part		Task part	
Variable name	Representation notation	Variable name	Representation notation
The collection of satellites	$S = \{S_1, S_2, \cdots, S_{N_S}\}$	The collection of tasks to be planned	$T = \{T_1, T_2, \cdots, T_{N_T}\}$
The collection of sorted tasks	$T_S = \{T_S^1, T_S^2, \cdots, T_S^n\}$	Geographic information	$\langle lla \rangle$
Image type of payload	H	Priority level	ω
Image spatial resolution	F	The collection of visible time periods	$W = \{[\text{sw}, \text{ew}]\}$
Energy	E	The earliest start and the latest end of imaging moment	est, let
The amount of stored data	G	Scheduled imaging periods	$\langle \text{set} \rangle = [\text{st}, \text{et}]$
Attitude maneuverability	Ac	Scheduled playback period	$\langle \text{seht} \rangle = [\text{sht}, \text{eht}]$
Attitude range	At	Image type requirements	h
Maximum imaging duration for one orbit	$t_{w-\max}$	Image resolution requirements	f
Replay period collection	$W' = \{[W'_s, W'_e]\}$	Minimum solar altitude angle	$\gamma_{\min}$

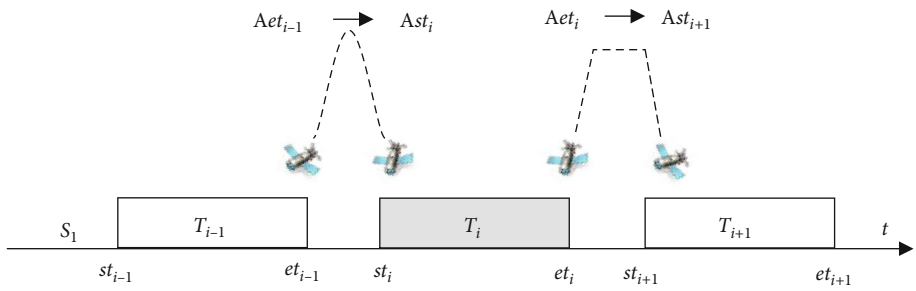

Figure 7: Attitude adjust between neighbor tasks.

(2) Task part

(i) Time constraint: the image task for S_j to T_i must be scheduled during the expected imaging time period and in the visible time collection W_{ij}. Playback activities should occur in the available playback part and does not precede the imaging action

$$\begin{aligned} &\langle \text{elt} \rangle = [\text{est}, \text{let}], \\ &\text{set}_i \subset W_{ij}, \text{set}_i \subset \text{elt}_i, \\ &\text{seht}_i \subset W'_{ij}, \text{sht}_i \leq \text{st}_i \end{aligned} \tag{10}$$

(ii) Imaging request constraint: the satellite payload type needs to match the image type and the resolution requirements of the task

$$H = h, F \geq f \tag{11}$$

(iii) Task revisit constraint: except multiple revisits request, the execution of tasks is unique

$$T_{Sj} \cap T_{Sl} = \varnothing \tag{12}$$

(iv) Solar altitude angle constraint: a typical optical task specifies the sun elevation angle γ range of the imaging to guarantee image quality

$$\gamma > \gamma_{\min} \tag{13}$$

3.3.2. Task Allocation Purpose. The multisatellite Earth observation mission planning process should meet the imaging constraints mentioned in Section 3.3.1; meanwhile, different planning schemes may be generated from different

Table 2: Main initial orbital elements of the satellite in simulation.

UTC time: 2018-06-01 10:30:00				
Orbital plane number	1	2	3	4
Satellite number	1 ~ 6	7 ~ 12	13~18	19~24
Semi-major axis (km)	7024.0	7124.0	7174.0	7224.0
RAAN (°)	256.5	346.5	166.5	76.5
True anomaly (°)		{0.0, 60.0, 120.0, 180.0, 240.0, 300.0}		

optimization angles, and the optimization target is usually given by the ground station. In order to simplify the solution complexity and highlight the task benefits in the dynamic environment, this work take the overall task efficiency of the system as the optimization goal of the algorithm as follows:

$$\max \sum_{j=1}^{N_S} \sum_{i=1}^{n_j'} \frac{1}{\omega_i}, \tag{14}$$

where ω_i is the priority of task T_i in I, which reflects the task importance, and n' is the number of payload task after planning the dynamic task T. The state of dynamic tasks changes rapidly over time, and the earlier the imaging, the greater the probability of high yield, so the yield probability function $P(rt_i)$ is introduced.

$$\begin{aligned} \mathrm{rt}_i &= \mathrm{et}_i - \mathrm{est}, \\ P(\mathrm{rt}_i) &= 1 - \frac{\mathrm{rt}_i}{\mathrm{let} - \mathrm{est}} = \frac{\mathrm{let} - \mathrm{et}_i}{\mathrm{let} - \mathrm{est}}, \end{aligned} \tag{15}$$

where rt_i is the task respond time, which reflects the response system speed to the task. The online earnings indicator after the introduction of $P(\mathrm{rt}_i)$ is as follows:

$$I : \max \sum_{j=1}^{N_S} \sum_{i=1}^{n_j'} \left(\frac{1}{\omega_i} \cdot \frac{\mathrm{let} - \mathrm{et}_i}{\mathrm{let} - \mathrm{est}} \right). \tag{16}$$

3.3.3. Optimization Model in Moving Target Allocation Method. Moving target online task planning problems can be seen as a type of online decision-making problem with real-time rolling updates of tasks, which need to be considered from the stage and the whole. The optimization is as follows:

(1) Overall purpose: in a fixed period of time, the higher the observation frequency of a moving target, the smaller the probability of tracking lost, and the higher the theoretical observation efficiency. Therefore, for the whole process of observation, the overall optimization goal is best time resolution RT

$$\begin{aligned} &I : \min \mathrm{RT} \longrightarrow \min \sim p, \\ &\mathrm{RT} = \frac{1}{n-1} \sum_{i=1}^{n-1} (\mathrm{et}_{i+1} - \mathrm{et}_i),\ 0 < i \le n, \end{aligned} \tag{17}$$

Table 3: Remote sensor simulation parameters.

Remote sensor parameters	Parameter settings
SAR incidence angle	10°~60°
$\gamma_{\min}$	20°
Optical remote sensor width/spatial resolution	100 km/15 m
SAR remote sensor width/spatial resolution	130 km/20 m
Hyperspectral remote sensor width/spatial resolution	50 km/20 m
Hyperspectral remote sensor spectral resolution	10 nm

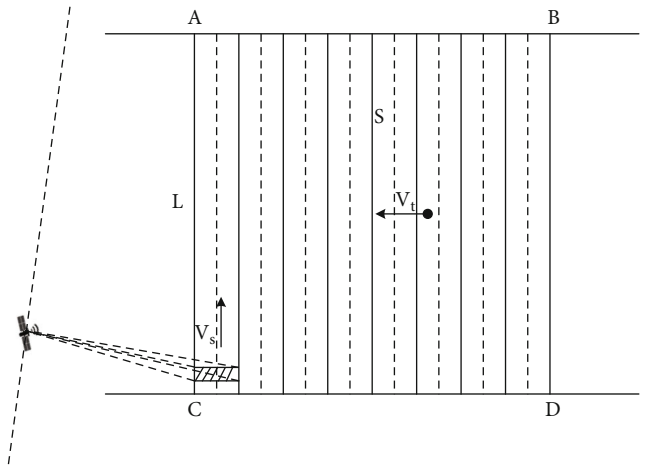

Figure 8: Observation model of swarm potential target search mission.

where n is the subtask executing times and $\sim p$ is the disappearance probability

(2) Single subtask stage objective: since the moving target has the highest priority, the observational benefit of the moving target subtask T_i is expressed as the best system's response speed rt to the subtask

$$\begin{aligned} &I' : \min \mathrm{rt} \longrightarrow \min A_i \longrightarrow \max p_i, \\ &rt = \mathrm{et}_i - \mathrm{est}_i,\ 0 < i \le n, \end{aligned} \tag{18}$$

where I' is the response of the overall goal in the subtask stage; the earlier the subtask time corresponds to the smaller the target potential area A_i, the greater the target discovering

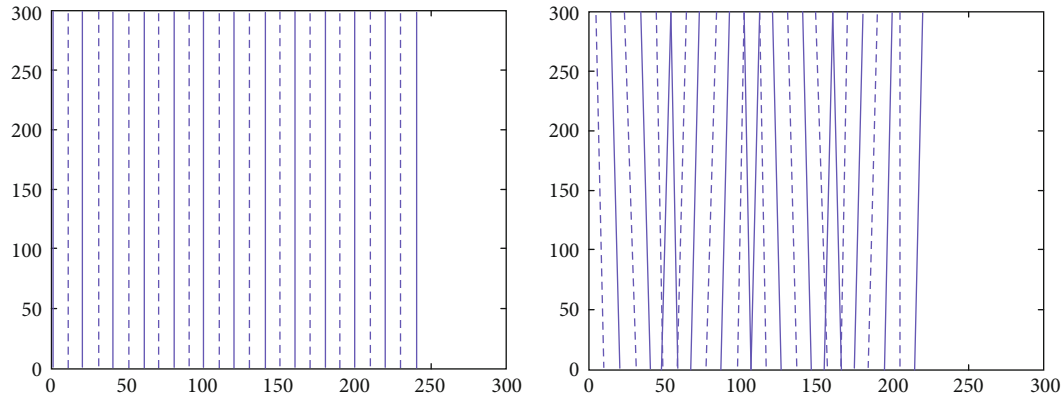

Figure 9: Different search strategies scheme.

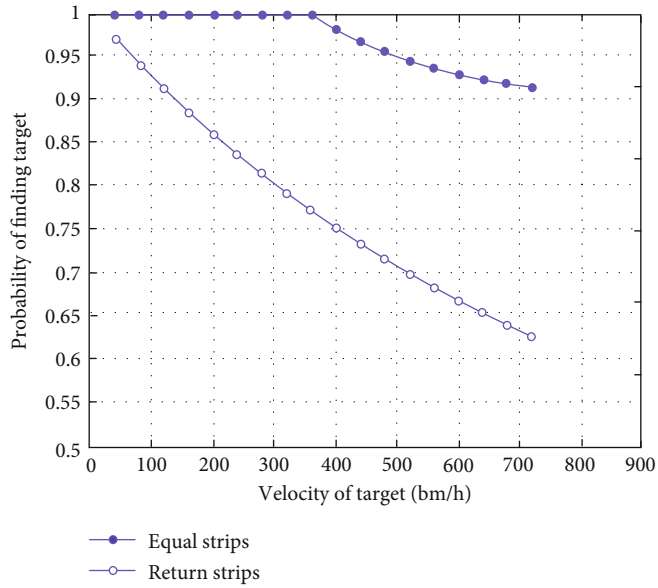

Figure 10: Probability of target discovery based-on different search strategies.

probability p_i. At the same time, the task is guaranteed to be executed as early as possible in the allocation process of each subtask, which will help reduce the time interval between tasks and is beneficial for improving the time resolution of the task, $I' \propto I$.

3.3.4. Optimization Model in Sensitive Target Allocation Method. Sensitive target task planning problems can be seen as an allocation problem combined with a specified time period and resource type. Besides the constraints given in Section 3.1, since the sensitive target must be observed multiple types of remote sensors $\{h\}$, the absence of an image type will let the task being unable to execute, the constraint is expressed as follows, where n denotes the total number of task performed for each type of satellite:

$$s.t.\{h\} = \bigcup_{i=1}^{n} H_i. \tag{19}$$

Time correlation needs to be considered during multitype image fusion, and the more similar the multisatellite imaging time, the higher the time correlation of the plan, and the higher the fusion images yield. Thus, the total execution efficiency for sensitive targets can be defined as the time similarity degree R of various images as follows:

$$\begin{aligned} R &= \max\ d\left(T_i, T_j\right), i, j \le n, i \ne j, \\ d\left(T_i, T_j\right) &= \left|\frac{\mathrm{st}_i + \mathrm{et}_i}{2} - \frac{\mathrm{st}_j + \mathrm{et}_j}{2}\right|, \end{aligned} \tag{20}$$

where d denotes the time period of any two different types of satellite missions, which is defined as the absolute value of the difference between the two imaging times due to the short execution time of the point target. R is the maximum of d, which represents the maximum time interval in times of imaging. Therefore, the smaller the R, the higher the

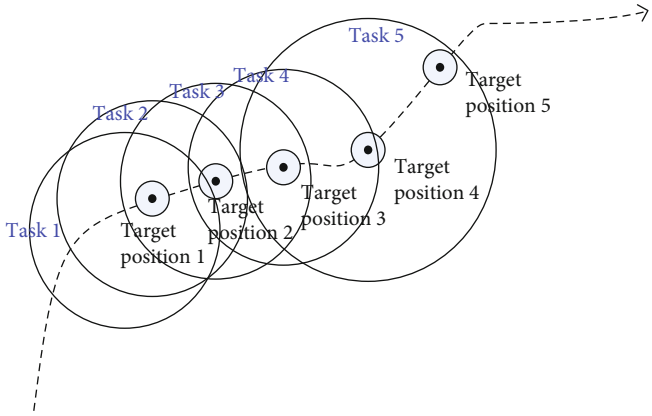

Figure 11: Observation model of swarm moving target tracking task.

image correlation degree is. Thus, the goal of the sensitive target task planning is the highest time correlation, and the purpose of the planning is to select a satellite with a similar imaging time for observation.

$$I = \min R = \min d\left(T_i, T_j\right). \tag{21}$$

4. Simulation of Self-Organizing and Assignment Process of Mission-Level Tasks

4.1. Simulation Environment. The simulation experiments are carried out on a computer with 4 G RAM. The designed satellite swarm earth observation system in this simulation includes 24 satellites: 4 orbital planes, and each orbital plane is distributed with 6 satellites, their orbital parameters are included in Table 2. Satellites are numbered as $6 \times O - 5 \sim 6 \times O$ (1 ~24), O is the orbital plane number. The even-numbered satellites carry SAR payloads, and the odd-numbered satellites carry optical payloads, with a ratio of 1 : 1. In Section 4.4, 8 satellites $(6 \times O - 2, 6 \times O - 4)$ are replaced with hyperspectral payload. The initial orbital elements and remote sensor simulation parameters are shown in Tables 2 and 3.

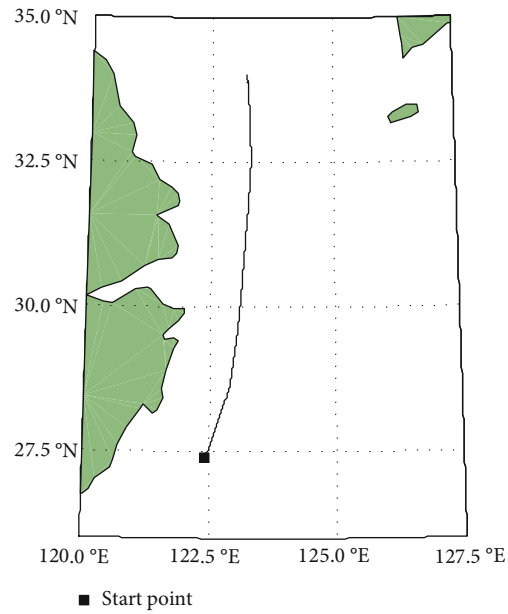

Figure 12: Ship's 24-hour trajectory setting.

4.2. Simulation of Task Allocation Process for Swarm Potential Target Searching. For the potential target searching task, a brief observation task model can be established, as shown in Figure 8. Suppose the area of concern is S, the satellite push-broom imaging direction length is L, the push-broom speed is V_s, and the maximum possible target moving speed is V_t. Considering that different types of satellites have different working modes, the push-broom direction of the satellite may be the direction shown in the figure or its reverse. At the same time, some satellites have agile imaging capabilities, that is, images of multiple strips can be acquired in one orbit, depending on the agile mobility of the satellite and the strip length L.

Since the initial position of the target in the area is unknown and the movement is unknown, the area must be searched in a full-coverage manner. But just covering the entire area is not enough. Since the coverage process is completed by multi-satellites, there is discontinuity. Between two observations, the target may move from an uncovered area to a covered area, causing the search to fail.

In response to the above problems, after the master satellite completes the strip segmentation and launches the task bidding, it needs to constantly repropose the time-constrained observation task requirements based on the completed coverage area and the worst estimation of the target motion, and the covered area entered need to be covered again. For example, as shown in Figure 9, assuming that the initial task bidding starts from the leftmost strip in the figure, the worst movement of the target is to move to the left. Therefore, the stripe range of the next bidding task should be considered to have a certain overlap with the previous one.

This self-organizing target search process is tested by simulation. Assuming that the target area has a length of 300 km in the east-west direction and 300 km in the north-south direction, several agile satellites are distributed in orbit, and there are different imaging directions. Assuming

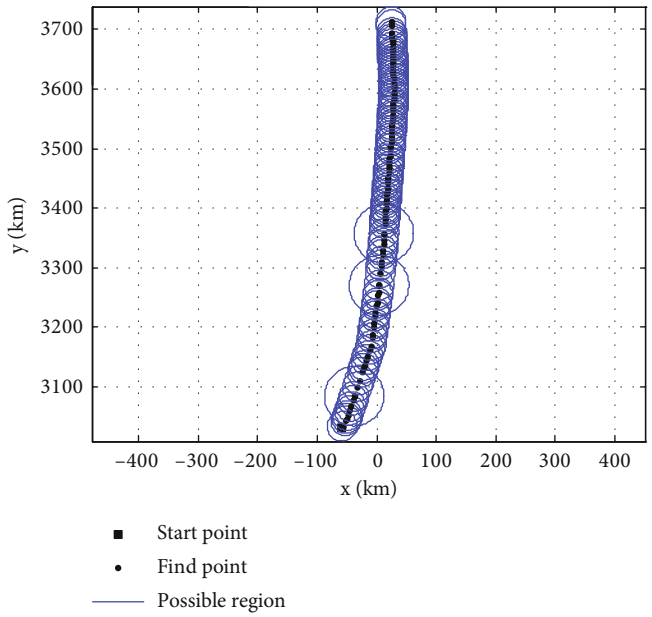

Figure 13: Simulation result of ship's 24-hour voyage tracking process.

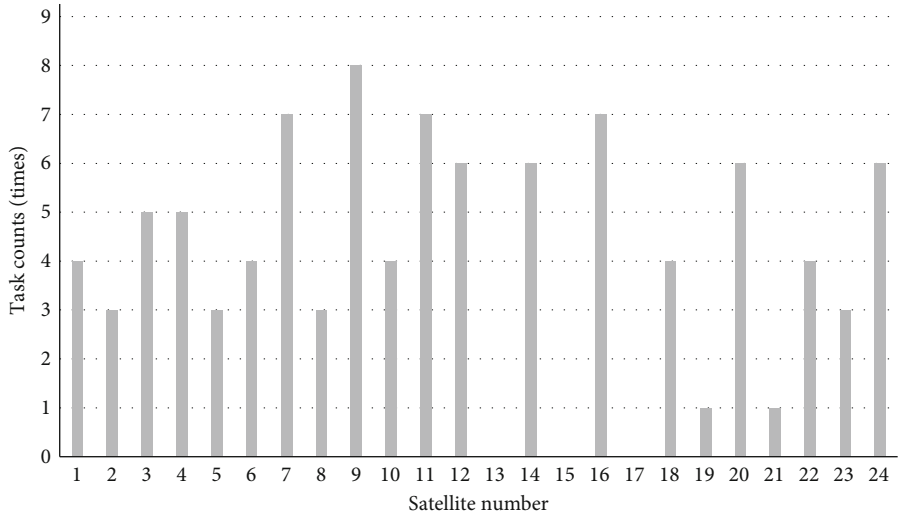

Figure 14: The result of the imaging task allocation of each satellite.

that the satellite has strong agility, it can complete 3 strips in one pass. At the same time, there are many satellites. After one satellite completes the imaging task, the next satellite can be immediately scheduled for imaging. Compare and analyze the effectiveness of two strategies: stripe equipartition search and stripe return search. The stripe equipartition search is shown in Figure 9(a), and the target area is divided into several stripes according to the satellite imaging width; the stripe return search is shown in Figure 9(b), and after the imaging is completed on the previous satellite, the next satellite is completely adjacent to the covered area at its push-broom starting point, and a horizontal search speed is added during the push-broom to form a certain overlap with the covered area.

This article assumes that the push-broom speed is 6 km/s, and the lateral search speed is 0.12 km/s. A large number of simulations are performed by randomly generating target positions to obtain the discovery probability of targets with different moving speeds, as shown in Figure 10.

It can be seen in Figure 10 that with the increase of target speed, the search strategy of stripe equalization reduces the probability of target discovery rapidly, while the stripe return search strategy can better maintain the ability to find the target. Combining the estimation of the target speed in orbit, by adjusting the return speed, the target can be fully discovered.

4.3. Simulation of Task Assignment Process for Moving Target Tracking. For moving target tracking tasks, limited

by the orbiting of satellites, it can only be achieved through intermittent, high-frequency imaging of different satellites. During each imaging time, what the satellite knows is only the potential area of the moving target. The potential area will become larger as the observation interval increases and is also affected by geographic conditions. These factors need to be considered when the master satellite is planning to track and imaging missions in orbit.

After the swarm receives the task of tracking and observing the moving target, the master satellite analyzes the potential area of the moving target and completes task assignment and planning through intersatellite negotiation. According to the task execution result, the recursive trajectory is used to predict the potential location range of the target, and new observation tasks are planned and assigned until the tracking task ends. The observation model of swarm moving target tracking task is represented in Figure 11.

Select the moving target as the ship for simulation test. Assuming that the maximum speed of the ship is 50 km/h, the swarm is configured with 4 orbital planes, and 6 satellites are distributed on each orbital plane, respectively, carrying visible optical or SAR payloads. The ship is found to be active in the sea at (27.4N, 122.4E) at 10:30:00 in the morning. Figure 12 contains the trajectory of the target 24 hours later.

After the tracking task is placed, the master satellite plans and initiates the tracking task. The simulation result of the tracking process is represented in Figure 13.

The task assignment and execution results of each satellite are in Figure 14.

The simulation results in Figure 14 show that imaging tasks are generated and auctioned 100 times; of which 97 tasks are executed with a potential area radius of 25 km; there are no satellite bids for the 3 tasks, and the potential area radius is expanded to 50 km. The cooperation of 24 satellites can complete a continuous day's tracking task, and the imaging quality is high.

The simulation analyzes the swarm of different scales and configurations and the continuous tracking ability of the target. Taking the moving target as above, under the same simulation conditions, adjust the number of orbital surfaces and the number of satellites on the orbital surface, and perform continuous tracking time simulation. The result is shown in Figure 15.

It can be seen in Figure 15 that when the number of orbital surfaces and the number of satellites is small, continuous tracking and observation throughout the day cannot be achieved. When the number of orbital surfaces is not less than 4, the average orbiting satellite is not less than 6, and at least 3 SAR satellites are included, continuous tracking and observation can be achieved throughout the day.

4.4. Simulation of Task Assignment for Sensitive Target Feature Confirmation. After the sensitive target is discovered by ground or earth observing system, it is uploaded to the swarm, and it is expected that the target characteristics can be identified and confirmed through the arrangement of serialized payload imaging tasks. For example, suppose that three types of payloads of A, B, and C are required to detect

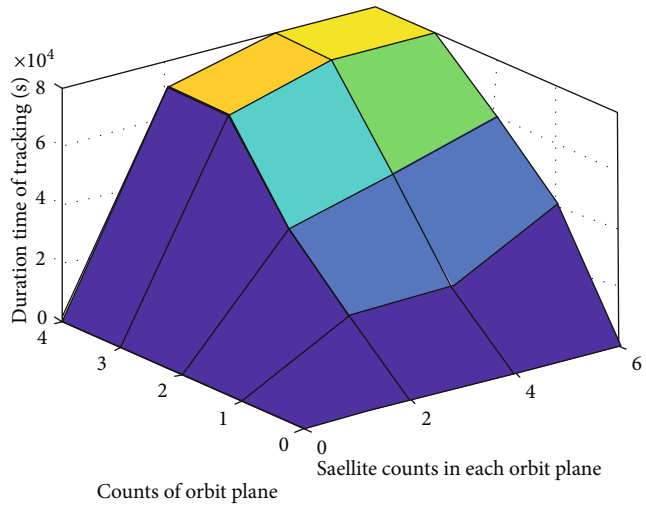

Figure 15: Simulation result of continuous tracking capabilities of swarms of different scales.

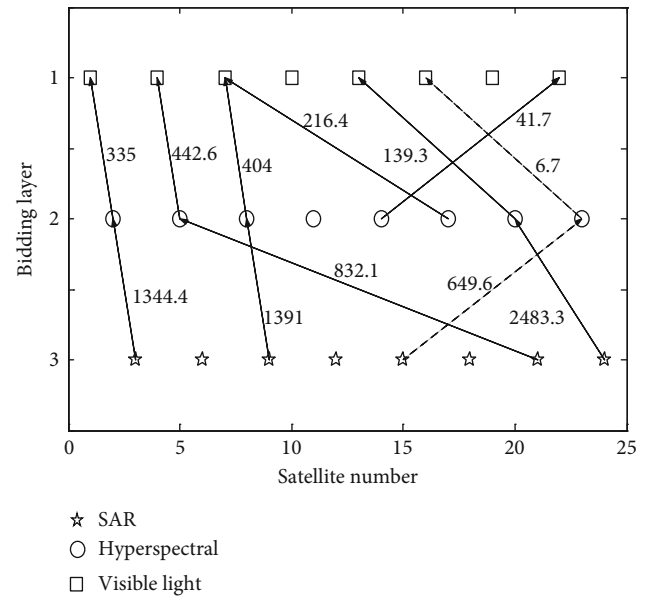

Figure 16: Group bidding model for sensitive target feature confirmation task.

and image the target in sequence, and the constraint condition is that the time interval between the three imaging operations is as short as possible to obtain the observation information of the target at the same time. Therefore, the task bidding process of the sensitive target feature confirmation task is multilayered and comprehensively optimized.

Multilayer, in accordance with the order of load types, the first layer of the A load is first tendered to form multiple bidding results. After that, in accordance with the principle of the closest time to the first-tier results, the bidding obtains the second-tier bidding results for the B-type load and forms several groups of team bidding results with directions. After analogy, the third-tier bidding result for the C-type load is obtained. Finally, the master satellite will evaluate the

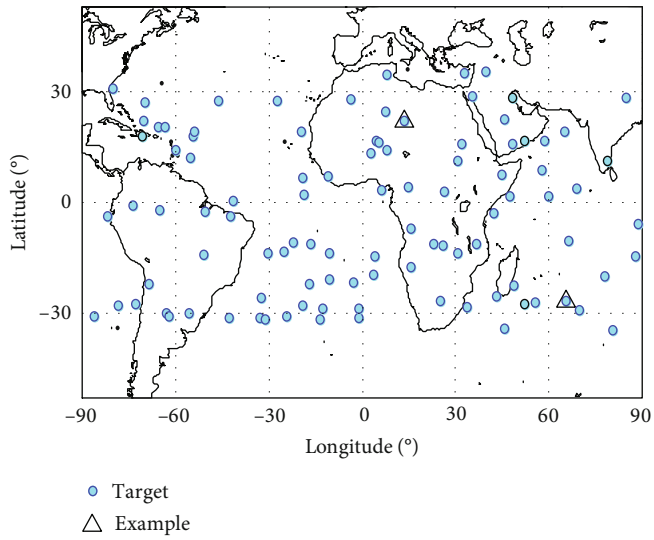

Figure 17: 100 groups of sensitive target distribution settings.

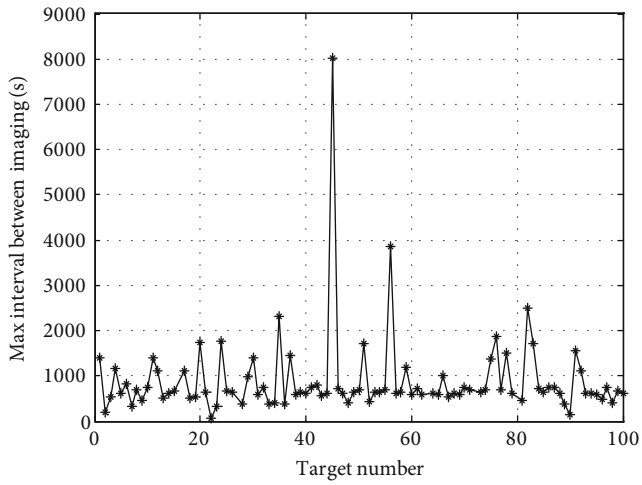

Figure 18: Simulation result of 100 groups of sensitive target observation.

effectiveness of all team bidding results. The evaluation criteria are the shortest task response time and the shortest team imaging process time. After three times of bidding, the bid-link result is represented in Figure 16.

The arrows in Figure 16 represent the bidding direction, and the marked numbers are time costs between the bidding plan and the directing plan. There are 5 complete bid link paths for this sensitive task. Using the bid evaluation method, iterate these paths from the third-tier back to select the optimal path $15 \longrightarrow 23 \longrightarrow 16$, which represented as the dotted line.

100-point targets are randomly generated on the map as sensitive targets, and 100 sets of experiments are performed, as shown in Figure 17. It is assumed that the designated bidding order of the target is visible light, hyperspectral, and SAR, and the team imaging time interval R is defined as the time interval between the first imaging and the last imaging, which represents the worst correlation of different types of images.

It can be seen from the Figure 18 that 5 targets are located in umbra during the planning period, and there is no visible optical satellite bidding, and the mission is directly abandoned. Therefore, the mission completion rate is 95%. Three targets are approaching the umbra during the planning period, and also affected by the scheduled high-level tasks, so that the team imaging time interval R is relatively large. The team imaging time interval R of most targets is below 1800s, with an average of 788.5 s. It can be concluded that, under suitable observation conditions, different targets can find a team of satellites within a closed imaging time through multisatellite negotiation to perform sequence observation tasks.

5. Conclusion

Large-scale swarm is the development trend of space-based earth observation system in the future. For swarm, mission-level task self-organization and collaboration techniques are important research topics, including potential target searching, moving target tracking, and target feature confirmation. This paper adopts the distributed task allocation method based on the improved contract network algorithm to realize the optimal allocation of inter-satellite tasks, that is, the mapping of swarm tasks from task space to execution space. Based on this, a mission-level task swarm coordination task allocation and planning process is designed, including some algorithms for the generation of observation requirements and the decomposition of observation tasks for different task types, as well as a common contract network allocation algorithm. Simulations are carried out on typical mission scenarios, focusing on the performance of different methods of potential target searching strategies, the effectiveness of tracking moving targets of different swarm scales, and the ability of multisatellite team bidding to complete sensitive target feature observation

tasks. Results verify that the improved contract network algorithm can solve the problem of optimizing the assignment of swarm mission-level observation tasks well and has potential in engineering application.

Data Availability

The data used to support the findings of this study are included within this paper.

Conflicts of Interest

The authors declare that there is no conflict of interest regarding the publication of this paper.

Acknowledgments

This work is supported in part by the project D020214, the Fundamental Research Funds for the Central Universities (No. 3072022JC0202).

References

[1] X. Yang, H. Mingren, S. Jiang, and L. Delin, "Attitude antagonistic consensus control of satellite swarm system based on MRPs," *Systems Engineering and Electronics*, vol. 43, no. 7, pp. 1904–1911, 2021.

[2] D. Izzo and L. Pettazzi, "Autonomous and distributed motion planning for satellite swarm," *Journal of Guidance, Control, and Dynamics*, vol. 30, no. 2, p. 449, 2007.

[3] A. Farrag, S. Othman, T. Mahmoud, and A. Y. ELRaffiei, "Satellite swarm survey and new conceptual design for Earth observation applications," *The Egyptian Journal of Remote Sensing and Space Science*, vol. 24, no. 1, pp. 47–54, 2021.

[4] H. Chuan, Z. Xiaomin, and Q. Dishan, "Cooperative scheduling method of multi-satellites for imaging reconnaissance in emergency condition," *Systems Engineering and Electronics*, vol. 34, no. 4, pp. 726–731, 2012.

[5] C. Yingwu, Y. Feng, and L. Jufang, "A learnable ant colony optimization to the mission planning of multiple satellites," *Systems Engineering - Theory & Practice*, vol. 33, no. 3, pp. 791–801, 2013.

[6] Z. Chao and L. Yanbin, "Planning and scheduling method for multi agile satellite coordinated mission," *Science Technology and Engineering*, vol. 17, no. 22, pp. 271–277, 2017.

[7] Z. Chao, L. Yuqing, F. Xiaoen et al., "A ground-onboard joint operation mechanism for the autonomous mission planning of imaging satellite cluster," *Journal of Harbin Institute of Technology*, vol. 50, no. 4, pp. 56–61, 2018.

[8] L. Xiaolu, H. Lei, C. Yingwu, and C. Yinguo, "An adaptive large neighborhood search algorithm for multiple agile satellites coordination and scheduling," *The Fourth China High Resolution Earth Observation Conference, Wuhan, September*, vol. 17, 2017.

[9] H. Chuanqi, L. Yurong, and L. Hu, "Mission planning for small satellite constellations based on improved genetic algorithm," *Chinese Journal of Space Science*, vol. 39, no. 1, pp. 129–134, 2019.

[10] H. Huicheng, J. Wei, L. Yijun, and Z. Yuan, "Research on agile satellite dynamic mission planning based on multi-agent," *Journal of National University of Defense Technology*, vol. 35, no. 1, pp. 53–59, 2013.

[11] C. Taoyi, F. Xiaoen, C. Jinyong, and L. Yuqing, "A multi-satellite autonomous coordination task planning method based on bidding mechanism," *Journal of Harbin Institute of Technology*, vol. 51, no. 4, pp. 138–145, 2019.

[12] Y. Longjiang, W. Xiande, M. Yilan, H. Gao, and Y. Hao, "Task allocation for distributed remote sensing satellites based on contract network algorithm," *Journal of Harbin Engineering University*, vol. 41, no. 7, pp. 1059–1065, 2020.

[13] W. Xiande, W. Bai, Y. Xie, X. Sun, C. Deng, and H. Cui, "A hybrid algorithm of particle swarm optimization, metropolis criterion and RTS smoother for path planning of UAVs," *Applied Soft Computing Journal*, vol. 73, no. 12, pp. 735–747, 2018.

[14] X. Sun, W. Xiande, W. Chen, Y. Hao, K. A. Mantey, and H. Zhao, "Dual quaternion based dynamics modeling for electromagnetic collocated satellites of diffraction imaging on geostationary orbit," *Acta Astronautica*, vol. 166, pp. 52–58, 2020.

[15] X. Wu, H. Zhao, B. Huang, J. Li, S. Song, and R. Liu, "Minimum-learning-parameter-based anti-unwinding attitude tracking control for spacecraft with unknown inertia parameters," *ACTA Astronautica*, vol. 179, pp. 498–508, 2021.

[16] X. Zhang, W. Zhu, X. Wu, T. Song, Y. Xie, and H. Zhao, "Dynamics and control for in-space assembly robots with large translational and rotational maneuvers," *Acta Astronautica*, vol. 174, pp. 166–179, 2020.

[17] Z. Zhu, Y. Luo, H. Wei et al., "Atmospheric light estimation based remote sensing image dehazing," *Remote Sensing*, vol. 13, no. 13, p. 2432, 2021.

[18] Z. Zhu, Y. Luo, G. Qi, J. Meng, Y. Li, and N. Mazur, "Remote sensing image defogging networks based on dual self-attention boost residual octave convolution," *Remote Sensing*, vol. 13, no. 16, p. 3104, 2021.

[19] H. Zhao, X. Wu, Y. Xie, Y. Du, Z. Zhang, and Y. Li, "Rotation matrix-based finite-time attitude synchronization control for flexible spacecrafts with unknown inertial parameters and actuator faults," in *ISA Transactions*, Elsevier, 2021.

[20] W. Zhou, Z. Xing, B. Wenbin, D. Chengchen, Y. Xie, and X. Wu, "Route planning algorithm for autonomous underwater vehicles based on the hybrid of particle swarm optimization algorithm and radial basis function," *Transactions of the Institute of Measurement and Control*, vol. 41, no. 4, pp. 942–953, 2019.